Int J Clin Exp Pathol 2013;6(7):1327-1336
www.ijcep.com /ISSN:1936-2625/IJCEP1304031

Original Article

Effects of human bone marrow mesenchymal stem cells on burn injury healing in a mouse model

Liang Xue, Ying-Bin Xu, Ju-Lin Xie, Jin-Ming Tang, Bin Shu, Lei Chen, Shao-Hai Qi, Xu-Sheng Liu

Department of Burns, The First Affiliated Hospital of Sun Yat-sen University, Guangzhou, 510080, Guangdong, P. R. China

Received April 23, 2013; Accepted May 21, 2013; Epub June 15, 2013; Published July 1, 2013

Abstract: Objective: To investigate the feasibility and safety of human bone marrow mesenchymal stem cells (BM-MSCs) transplantation on the improvement of burn wound healing. Method: Human BM-MSCs were injected into the skin of the mouse models, and the new blood vessels growth, the engraftment of BM-MSCs and the speed of healing were observed. Moreover the body weight and activity were tested after BM-MSCs transplantation. Results: We found that wound surface healing was significantly accelerated when BM-MSCs were applied to the wound surface in mice. Moreover, both the number and density of new blood vessels were increased in the BM-MSC-treated group. The engraftment of BM-MSCs was also investigated using GFP-labeled cells and no GFP-positive cells were observed in tissues other than the location of BM-MSC injection. We also found that both body weight and activity were quickly restored in BM-MSC-treated mice, and no tumor growth was found. Conclusion: The present results suggest that BM-MSC transplantation can effectively improve wound healing in a mouse model of burn injuries. Use of BM-MSCs might therefore facilitate development and improvement of burn injury treatments in future.

Keywords: Bone marrow mesenchymal stem cells, burn injury, wound healing, mouse model

Introduction

Burn injuries constitute a major worldwide public health problem and cause more severe physiological stress than other traumas. Burn injuries to skin result in loss of its protective function as a barrier to micro-organisms, leading to a high risk of infection, therefore effective treatment and healing of burn injuries are very important to prevent complications [1]. Burn injury healing is a complex physiological process, which includes numerous biological and molecular events such as cell migration and proliferation, extracellular matrix (ECM) deposition, angiogenesis and remodeling. In addition to traditional clinical treatments, new methodologies to promote burn injury healing mainly depend on 3-dimensional reconstruction to facilitate angiogenesis and epithelial propagation [2], and to reduce inflammation; however, the effects are not desirable. Therefore, it is important to explore new methods to reduce the harm caused by burn injuries in humans.

Mesenchymal stem cells (MSCs) are multipotent adult stem cells which are abundant in human tissue. MSCs are classified in accordance with their tissue of origin, for example bone marrow MSCs (BM-MSCs), umbilical cord MSCs and adipose MSCs. It has been proven that MSCs can be propagated *in vitro* and retain their multipotency through multiple passages. Moreover, MSCs can differentiate into adipose tissue, bone, cartilage, muscle, neurons, liver cells and cardiocyte, among other cell types [3, 4]. Among these MSCs, BM-MSCs are thought to play a key role in wound healing. Falanga *et al*. reported that autologous BM-MSCs in a fibrin spray system could accelerate healing in murine and human cutaneous wounds [5], and this was also proved by other studies [6, 7]. BM-MSCs thus show tremendous potential to improve wound healing; however, to the best of our knowledge, there are no reports on the use of BM-MSC to treat burn injuries.

In the present study, we examined the feasibility and safety of BM-MSC transplantation to

improve healing of burn injuries in a mouse model. Green fluorescence protein (GFP)-expressing allogeneic MSCs were implanted into wounds in a mouse model, and wound healing was evaluated by assessing wound surface healing efficiency, angiogenesis and capillary density.

Materials and methods

In the present study, all chemicals were purchased from Sigma Aldrich Co. (Shanghai, China), unless otherwise indicated.

Ethical approval

This study was approved by the Institutional Review Board of Sun Yat-sen University. Mice were handled in strict accordance with the Guidelines for the Care and Use of Laboratory Animals of Sun Yat-sen University, and the protocol was approved by the Institutional Review Board of Animal Experiments of Sun Yat-sen University.

Derivation of human BM-MSCs

With the written consent of healthy donors, 5–10 mL of bone marrow was obtained from the ilium by biopsy. Bone marrow was diluted with the same volume of phosphate-buffered saline (PBS) after heparin treatment. After centrifugation (300 × g, 4 min) in Ficoll lymphocyte separation solution and rinsing twice with PBS, the cells in the middle layer were collected and cultured in a cell-culture dish. The dissociated mesenchymal cells were further dispersed in 10% FBS-DMEM and counted under a microscope with the aid of a hemocytometer. The mesenchymal cells were then used directly for culture or stored in liquid nitrogen for later use.

GFP transfection

MSCs at passage 4 were transfected with a human lentivirus carrying GFP reporter genes. The GFP gene was first linked to a human lentivirus vector, and packaged by 293T cells. Lentivirus was produced by the ultracentrifugation method. MSCs were then plated into six-well plates and cultured in a humidified atmosphere at 37°C with 5% CO_2. When the cells reached 70% confluence the medium was removed and replaced with culture medium supplemented with GFP lentivirus. The cells were cultured in a humidified atmosphere for 6–12 h at 37°C with 5% CO_2, and observed under a fluorescence microscope after 24–48 h. The transfected cells were passaged when they reached 80–90% confluence.

Fluorescence-activated cell sorting and culture of sorted cell populations

BM-MSCs were harvested and dissociated in cell dissociation buffer (Gibco). Dissociated single cells were stained with phycoerythrin (PE)-conjugated antibodies. Sorted CD45-positive cells and CD9-negative cells were co-cultured with OP9 stromal cells at a cell density of 2×10^3/well in 24-well plates. In contrast to previous reports, differentiation of MSCs as a result of FAC sorting was not observed in this study. The above experiments were repeated 10 times.

Mouse model of burn injury

In this study, male mice of the outbred strain ICR at 8–10 weeks of age were used, to avoid variability as a result of the female estrous cycle. Mice were housed and bred at the Animal Center of Sun Yat-sen University in line with national legislation covering animal care. All mice were maintained individually under controlled temperature and lighting conditions with food and water supplied *ad libitum*.

Mice were anesthetized by intraperitoneal injection of 40 mg/kg pentobarbital sodium. The fore limbs of each mouse were subjected to a nonlethal scald injury, representing 3–5% total body surface area, by immersion in 90°C water for 3 s. The mice were divided into two groups; in the experimental group, BM-MSCs were injected into the scalded hind limbs, while the control group received identical injections of growth-factor reduced Matrigel/PBS minus the BM-MSCs. For BM-MSC treatment, the cells were resuspended in 1 mL α-MEM at a concentration of 1×10^7 cells/mL. Each wound received 1 million cells (GFP-BM-MSCs): 0.7×10^6 in 60 μL of PBS injected intradermally around the wound at four injection sites and 0.3×10^6 in 20 μL of growth factor-reduced Matrigel (BD Biosciences) applied to the wound bed [6].

Wound healing time and efficiency

The burn wounds were observed daily, and when the wound was completely covered by

Table 1. PCR primers used to detect gene expression in wound samples

Gene	Sense	Antisense	Size (b.p.)
HLA-B2704	GGGTCTCACACCCTCCAGAAT	CGGCGGTCCAGGAGCT	135
HLA-DQB-1-0201	GTGCGTCT TGTGAGCAGAAG	GCAAGGT CGT GCGGAGCT	205
Ang-1	GGGTCTCACACCCTCCAGAAT	CGGCGGTCCAGGAGCT	135
Ang-2	GTGCGTCT TGTGAGCAGAAG	GCAAGGT CGT GCGGAGCT	205
CD31	GGGTCTCACACCCTCCAGAAT	CGGCGGTCCAGGAGCT	135
VEGF	GTGCGTCT TGTGAGCAGAAG	GCAAGGT CGT GCGGAGCT	205

newly-formed epithelium it was regarded as healed. The wound area was identified by transparent film tracing and weighting methods. The efficiency of wound healing was calculated following the formula:

Rate of wound healing = [(original wound area – unhealed wound area)] / original wound area × 100%

RNA isolation and reverse transcription

New tissues were collected and used for RT-PCR analysis. The above tissues were ground up and washed twice in warm PBS, then dissociated with 0.5% trypsin. Cells were spun down and washed in cold PBS, then RNA was isolated using Trizol (Invitrogen, Carlsbad, CA) according to the manufacturer's protocol. Aliquots containing 1–2 μg purified total RNA were treated with amplification grade DNase I (Invitrogen) according to the manufacturer's protocol, and 250 ng RNA was used for a reverse transcription reaction using the SuperScript II system (Invitrogen) by combining 1 μL random hexamer oligonucleotides (Invitrogen), 1 μL 10 mM dNTP (Invitrogen), and 11 μL RNA plus water. This mixture was brought to 70°C for 5 minutes, and then cooled to room temperature. SuperScript II reaction buffer, DTT (Invitrogen) and SuperScript II were then added according to the manufacturer's protocol and the mixture was warmed to 25°C for 5 minutes, 42°C for 50 minutes, 45°C for 20 minutes, 50°C for 15 minutes and 70°C for five minutes. HLA-B2704 and HLADQB1-0201 genes were used to identify human MSCs to assess survival and propagation after transplantation. The primers used are shown in **Table 1**.

Relative mRNA expression

Relative mRNA expression of Ang-1/2, CD31 and VEGF genes was analyzed using qRT-PCR. Total RNA was isolated using a miRNeasy Mini kit (Qiagen) and subjected to on-column DNase digestion according to the protocol. To validate changes in gene expression, RNA was converted to cDNA, and qPCR was carried out according to the manufacturer's instructions (Applied Biosystems 7500). In each experiment, a sample without reverse transcriptase and a sample without template were included to demonstrate specificity and lack of DNA contamination. The primers used are shown in **Table 1**.

Calculation of capillary density

Samples of approximately 2 mm^3 were obtained from the MSC-transplanted and the control mice. The tissues were fixed using 10% formalin and stained with hematoxylin and eosin. Tissue sections were observed under a light microscope. A total of eight sections were observed from each mouse and ten images were selected under a 40 × field of vision. The number of capillaries was counted using the CMIAS software, and the average number was calculated.

MSC migration

The mice were killed by suffocation, and tissues were collected quickly and prepared for cryosectioning. Frozen sections, 30 μm in thickness, were cut of tissues including heart, liver, spleen, pancreas, lung, kidney, intestine, brain, peritoneum and eyes. GFP cells were observed by confocal microscopy (LSM 510, ZEISS).

Body weight

Mice in both groups were weighed weekly and the body weights were recorded.

Pole test

Ten mice were used for a climbing test. Their performance was examined on a vertical pole

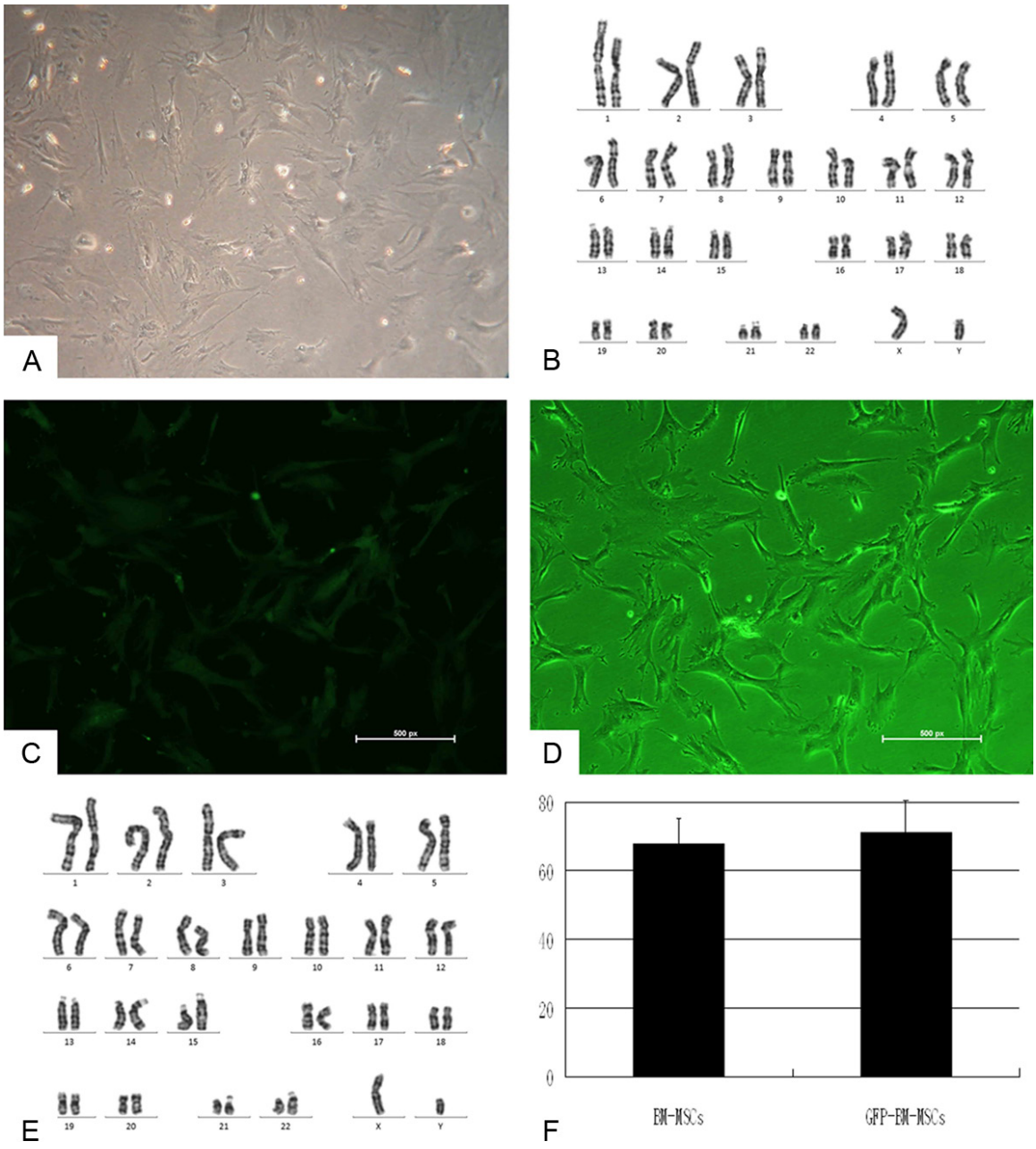

Figure 1. Characteristics of BM-MSCs before and after GFP transfection. A. BM-MSCs at passage 2. B. Karyotyping of BM-MSCs at passage 5. C. GFP BM-MSCs under a fluorescence microscope. D. BM-MSCs under a light microscope. E. Karyotyping of GFP BM-MSCs at passage 10. F. Doubling time analysis of BM-MSCs before and after GFP transfection.

(1 cm in diameter, 60 cm in height) at 12 and 20 weeks after implantation in each group. Mice placed on a vertical pole turned downwards and descended the pole. Mice were habituated to this task after 2 trials per day for 2 days. On the test day (day 3) 3 assessments were taken over 5 trials per mouse: the total time taken to descend, the time taken to turn and the time taken to descend after turning.

Statistical analysis

Student's paired t test was used to compare data of paired samples. All values are expressed

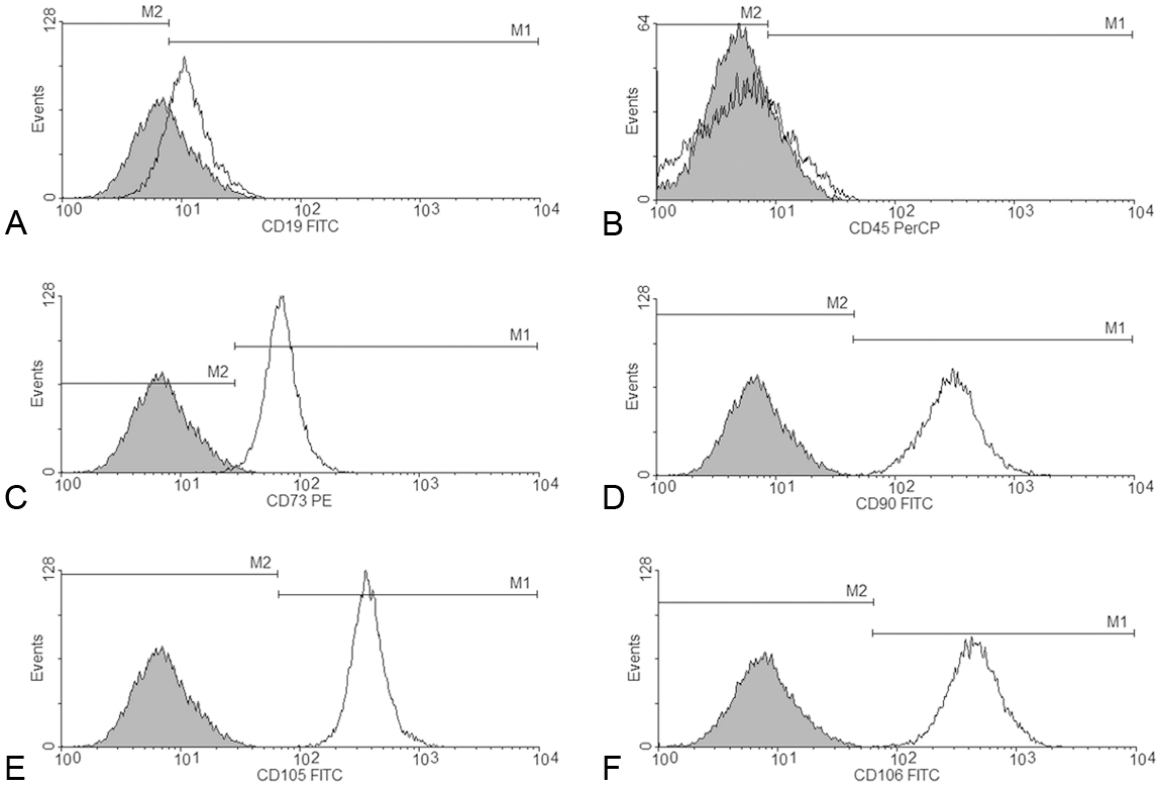

Figure 2. Flow cytometric analysis of specific negative and positive cell surface markers of BM-MSCs. A. Negative marker, CD19; (B) Negative marker, CD45; (C) Positive marker, CD73; (D) Positive marker, CD90; (E) Positive marker, CD105; (F) Positive marker, CD106.

as mean ± SD. A *P* value less than 0.05 was considered significant.

Results

Derivation of BM-MSCs

Bone marrow was collected from six donors, and five BM-MSC lines were successfully derived from them after primary culture. These five cell lines were propagated *in vitro* for more than twenty passages, and were named BM-MSC-1, -2, -3, -4 and -5. The cells showed normal spindle-shaped morphology, and maintained a normal karyotype (**Figure 1A** and **1B**).

At passage 4, BM-MSC-1, -2, -3, -4 and -5 cells at 60–70% confluence were transfected with GFP lentivirus, and GFP-positive cells were screened by FACS (**Figure 1C** and **1D**). The results of doubling-time analysis and karyotyping indicated that GFP transfection of BM-MSCs would not impair propagation (**Figure 1E** and **1F**).

Identification of specific markers of BM-MSCs

Specific markers were identified and analyzed by FACS. BM-MSCs were negative for CD19 and CD45 (**Figure 2A** and **2B**), but CD73, CD90, CD105 and CD106 were strongly expressed (**Figure 2C-F**).

Effects of BM-MSC implantation on wound healing

Escharectomy was performed on 60 burn wounds on day 3 after injury (30 mice in the BM-MSC group and 30 mice in the control group). In the BM-MSC group, 37.88% of the wound surface had healed by day 7 and 68.32% by day 14, but in the control group, wound surface healing efficiency only reached 30.43% on day 7 and 54.23% on day 14, significantly lower than the BM-MSC group. Accordingly, all wounds in the BM-MSC group were healed by day 20, which was significantly faster than in the control group (healing time 25 days on average) (**Figure 3A**).

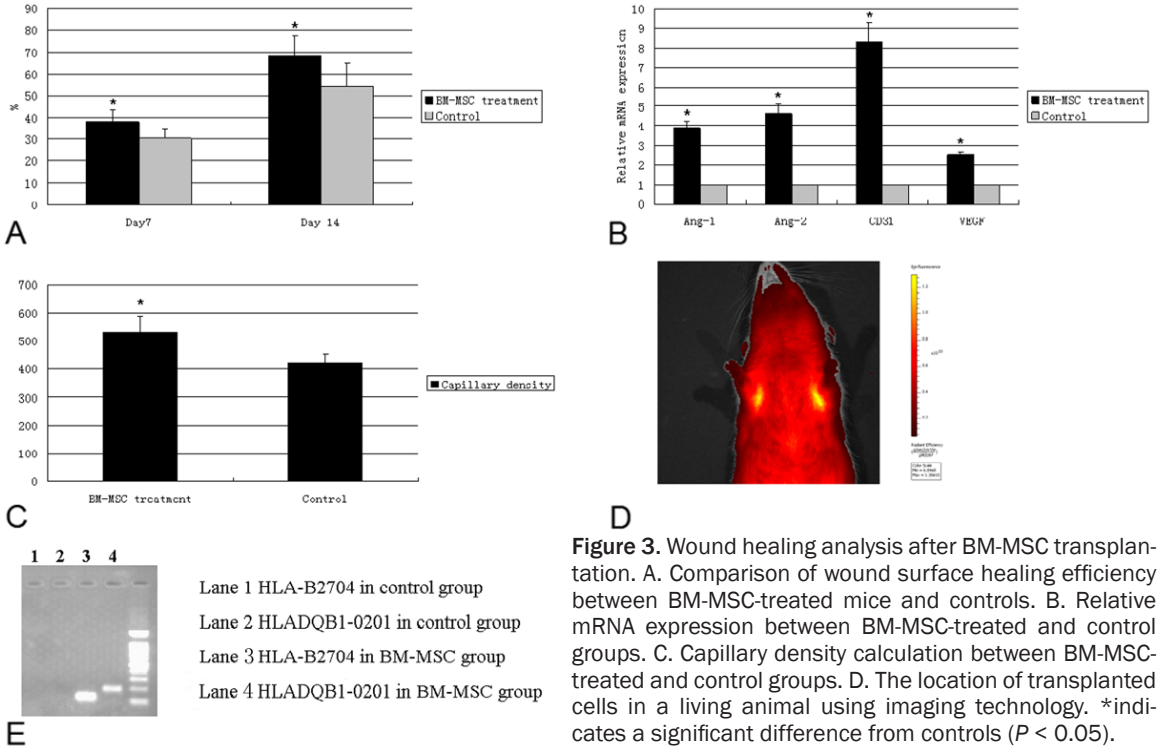

Figure 3. Wound healing analysis after BM-MSC transplantation. A. Comparison of wound surface healing efficiency between BM-MSC-treated mice and controls. B. Relative mRNA expression between BM-MSC-treated and control groups. C. Capillary density calculation between BM-MSC-treated and control groups. D. The location of transplanted cells in a living animal using imaging technology. *indicates a significant difference from controls ($P < 0.05$).

Angiogenesis is a key index of wound healing. In the BM-MSC group, vessels and fine branches could be observed by the naked eye and simple networks were formed, but these were difficult to see in the control group. We also investigated expression of specific markers of new vessels. Results of RT-PCR and western blotting showed that Ang-1/2, CD31 and VEGF were expressed in both the BM-MSC and control groups, but expression of these 4 genes was much stronger in the BM-MSC group (**Figure 3B**). Moreover, capillary density was calculated in both groups. In the BM-MSC group, the density was 532/mm^2, which was significantly higher than in the control group (425/mm^2) (**Figure 3C**). GFP-positive signals were observed distributed around the burn injury on day 7 in the BM-MSC group (**Figure 3D**), and RT-PCR results showed that HLA-B2704 and HLADQB1-0201 genes, expressed specifically in human cells, were detected in the wound tissues (**Figure 3E**).

Effects and safety evaluation of BM-MSC implantation

To evaluate the safety of BM-MSC implantation, the body weight and activity of the mice in the BM-MSC (n = 32) and control (n = 38) groups were tested. Body weight in the BM-MSC group was significantly lower than that of normal mice in the first 6 weeks after MSC treatment, but it became similar by the beginning of the 7th week. However, body weight in the control group remained significantly below that of normal mice throughout the first 9 weeks, and only became similar by the 10th week (**Figure 4A**).

At 12 weeks after MSC implantation, climbing activity was tested. The average time for which a mouse stayed at the top of the pole was 18 s and the time taken from top to bottom was 25 s in the BM-MSC group, but was significantly longer in the control group (26 s and 40 s, respectively). At 20 weeks after MSC implantation, climbing activity was tested again. The average time for which a mouse stayed at the top of the pole was 12 s and the time taken from top to bottom was 17 s in the BM-MSC group and these results were not significantly different compared to the control group (14 s and 18 s, respectively) (**Figure 4B** and **4C**).

Thirty mice were dissected at 24 weeks after BM-MSC implantation, and no GFP-positive cells were observed in other tissues, including the lung, heart, kidney, liver, brain, and pancreas (**Figure 5A-F**). Moreover no tumor or other pathological changes could be observed under an optical microscope (**Figure 5A1-F1**).

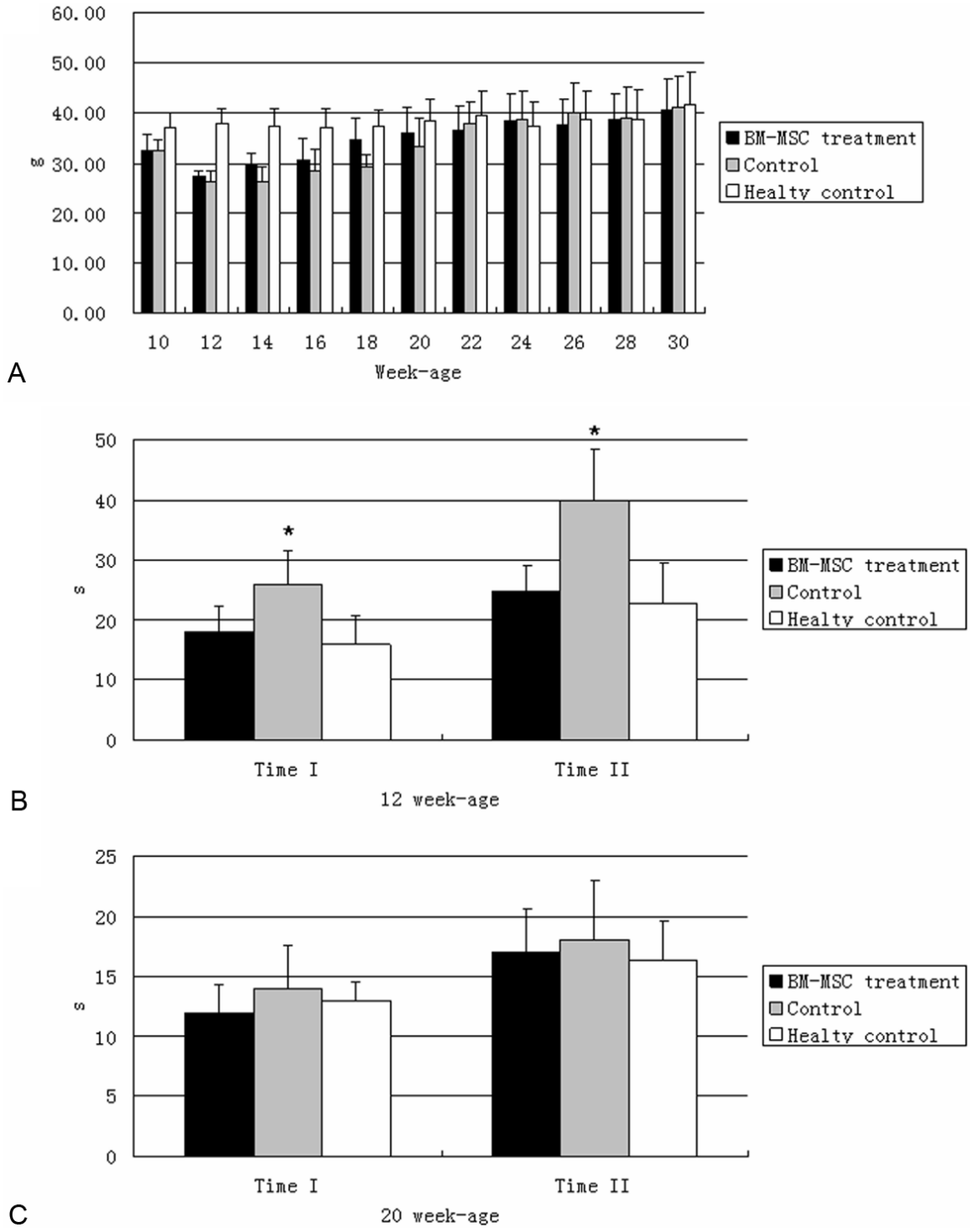

Figure 4. Effects of BM-MSC transplantation in the burn injury mouse model. A. Body weight from 10 to 30 weeks of age. B. Analysis of pole-climbing time of burn injury mice at 12 weeks after BM-MSC transplantation. C. Analysis of pole-climbing time of burn injury mice at 20 weeks after BM-MSC transplantation.

Discussion

In the present study, we show that BM-MSCs may improve burn injury healing in mice. Implantation of BM-MSCs significantly accelerated wound closure by increasing the rates of wound surface healing and angiogenesis, while the body-weight of mice treated with BM-MSCs

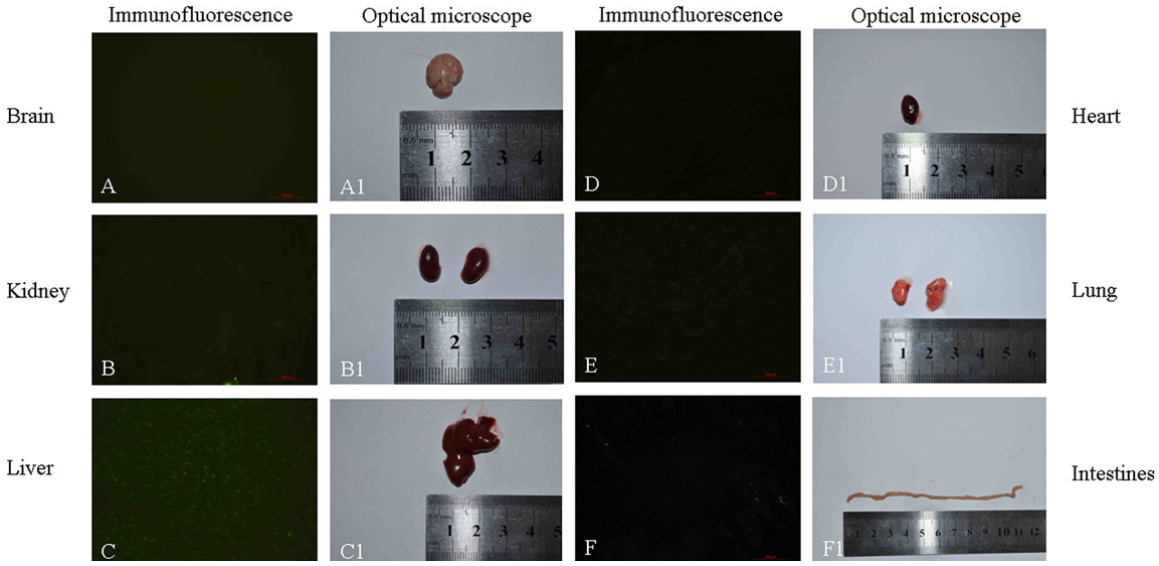

Figure 5. Risk evaluation of BM-MSC transplantation in the burn injury mouse model. A. Brain, (B) kidney, (C) liver, (D) heart, (E) lung and (F) intestines under a fluorescence microscope; (A1) Brain, (B1) kidney, (C1) liver, (D1) heart, (E1) lung and (F1) intestines under a light microscope.

was restored more quickly and they also displayed much better mobility compared to the control group. Furthermore, the safety of BM-MSC implantation was also demonstrated by the engraftment of BM-MSCs into wound skin, as well as by pathological analysis of a range of other tissues.

Although MSCs are actually present in many other tissues [8-10], mesenchymal stem cells (MSCs) are non-hematopoietic cell precursors initially found in bone marrow [11]. MSCs are relatively rare in the bone marrow ($1/10^5$ mononuclear cells), but they can proliferate very efficiently while preserving their stem cell properties *in vivo*. The progressive loss of differentiation potential due to senescence generally occurs after long-term propagation [12-14]. Although BM-MSCs display characteristics of multi-potent stem cells, there is still a lack of specific markers to identify them. In our study, 6 markers were identified by FACS. BM-MSCs were also labeled with GFP to track the cells after implantation. Whether or not GFP lentivirus transfection has a detrimental effect on the properties of BM-MSCs is not known, but in an embryo study, Niu *et al.* indicated that GFP transfection did not affect embryo developmental competence [15]. In the present study, we also compared BM-MSCs with GFP-BM-MSCs, and our results indicated no differences in differentiation *in vitro*, in specific cell marker expression or in doubling time, suggesting that GFP would not affect the developmental potential of BM-MSCs.

Several clinical trials using MSCs have been performed, including for the treatment of neurological diseases [16], spinal injury [17], and myocardial infarction [18, 19]. Although several reports have demonstrated some efficacy of MSCs, whether MSCs contribute significantly to regeneration of damaged tissue by tissue-specific transdifferentiation remains controversial. In our study, green fluorescence could still be observed when the burn injury was healed, indicating that BM-MSCs differentiate into the epidermis of the skin, while angiogenesis also indicated that BM-MSCs could contribute to blood vessel formation. Moreover, previous studies in wound healing have shown that BM-MSCs are recruited into wounded skin and contribute to wound repair by transdifferentiation into multiple skin-cell types [20, 21]. Of course the microenvironment would also influence the outcome of BM-MSC treatment and a biologically complete tissue would not form when the microenvironment is unsuitable. Physiological accumulation of sufficient MSCs might also induce further cell type differentiation, resulting in better functional organization of the wounded tissue. Although the mechanism of transdifferen-

tiation of MSCs has been vigorously investigated, sufficient progress has not been made to allow for its use in clinical applications.

The greatest advantage of BM-MSC treatment is that BM-MSCs have no or limited immunogenicity. BM-MSCs can not only survive homogeneously, but also heterogeneously, and maintain multi-differentiation competence [22]. In the present study, human BM-MSCs were transplanted into mouse models, and grew without tumor formation. Some studies demonstrated that a lower density distribution of MHC-1 antigen, and less expression of MHC-II antigen and stimulating factors, contribute to absent or lower immunogenicity [23, 24]. The regular molecular mechanism underlying the effect of MSCs on immunogenicity is that they inhibit T and B cell proliferation, but not T cell activity. Moreover, MSCs also inhibit NK cell proliferation, and reduce secretion of TNF-α and IL-10 [25, 26]. Since they are a type of immunodeficient cell, it is almost impossible to conduct immunological rejection without strict pairing, which increases the prospects of transplantation treatment to treat wounds and in regenerative medicine.

In summary, we demonstrate the treatment potential of human BM-MSCs for burn injuries in mice. Our results, taken together with the results of previous studies as well as several clinical trials using MSCs to treat injuries including spinal injury and myocardial infarction, show that BM-MSCs facilitate regenerative medicine and will promote cell therapy in future.

Address correspondence to: Dr. Xu-Sheng Liu, Department of Burns, The First Affiliated Hospital of Sun Yat-sen University, Guangzhou, 510080, Guangdong, P. R. China. Phone: +86-20-81122388; E-mail: liuxusheng7984@126.com

References

[1] Singer AJ and Clark RA. Cutaneous wound healing. N Engl J Med 1999; 341: 738-746.

[2] Pardue EL, Ibrahim S and Ramamurthi A. Role of hyaluronan in angiogenesis and its utility to angiogenic tissue engineering. Organogenesis 2008; 4: 203-214.

[3] Kastrinaki MC, Andreakou I, Charbord P and Papadaki HA. Isolation of human bone marrow mesenchymal stem cells using different membrane markers: comparison of colony/cloning efficiency, differentiation potential, and molecular profile. Tissue Eng Part C Methods 2008; 14: 333-339.

[4] Al-Nbaheen M, Vishnubalaji R, Ali D, Bouslimi A, Al-Jassir F, Megges M, Prigione A, Adjaye J, Kassem M and Aldahmash A. Human Stromal (Mesenchymal) Stem Cells from Bone Marrow, Adipose Tissue and Skin Exhibit Differences in Molecular Phenotype and Differentiation Potential. Stem Cell Rev 2013; 1: 132-43.

[5] Falanga V, Iwamoto S, Chartier M, Yufit T, Butmarc J, Kouttab N, Shrayer D and Carson P. Autologous bone marrow-derived cultured mesenchymal stem cells delivered in a fibrin spray accelerate healing in murine and human cutaneous wounds. Tissue Eng 2007; 13: 1299-312.

[6] Wu Y, Chen L, Scott PG and Tredget EE. Mesenchymal stem cells enhance wound healing through differentiation and angiogenesis. Stem Cells 2007; 25: 2648-2659.

[7] Mackenzie TC and Flake AW. Human mesenchymal stem cells persist, demonstrate site-specific multipotential differentiation, and are present in sites of wound healing and tissue regeneration after transplantation into fetal sheep. Blood Cells Mol Dis 2001; 27: 601-604.

[8] Bieback K and Kluter H. Mesenchymal stromal cells from umbilical cord blood. Curr Stem Cell Res Ther 2007; 2: 310-323.

[9] Lu LL, Liu YJ, Yang SG, Zhao QJ, Wang X, Gong W, Han ZB, Xu ZS, Lu YX, Liu D, Chen ZZ and Han ZC. Isolation and characterization of human umbilical cord mesenchymal stem cells with hematopoiesis-supportive function and other potentials. Haematologica 2006; 91: 1017-1026.

[10] Maharlooei MK, Bagheri M, Solhjou Z, Jahromi ZM, Akrami M, Rohani L, Monabati A, Noorafshan A and Omrani GR. Adipose tissue derived mesenchymal stem cell (AD-MSC) promotes skin wound healing in diabetic rats. Diabetes Res Clin Pract 2011; 93: 228-234.

[11] Prockop DJ. Marrow stromal cells as stem cells for nonhematopoietic tissues. Science 1997; 276: 71-74.

[12] Madeira A, da Silva CL, dos Santos F, Camafeita E, Cabral JM and Sa-Correia I. Human mesenchymal stem cell expression program upon extended ex-vivo cultivation, as revealed by 2-DE-based quantitative proteomics. PLoS One 2012; 7: e43523.

[13] Schellenberg A, Lin Q, Schuler H, Koch CM, Joussen S, Denecke B, Walenda G, Pallua N, Suschek CV, Zenke M and Wagner W. Replicative senescence of mesenchymal stem cells causes DNA-methylation changes which correlate with repressive histone marks. Aging (Albany NY) 2011; 3: 873-888.

[14] Wagner W, Horn P, Castoldi M, Diehlmann A, Bork S, Saffrich R, Benes V, Blake J, Pfister S, Eckstein V and Ho AD. Replicative senescence of mesenchymal stem cells: a continuous and organized process. PLoS One 2008; 3: e2213.
[15] Niu Y, Yu Y, Bernat A, Yang S, He X, Guo X, Chen D, Chen Y, Ji S, Si W, Lv Y , Tan T, Wei Q, Wang H, Shi L, Guan J, Zhu X, Afanassieff M, Savatier P, Zhang K, Zhou Q and Ji W. Transgenic rhesus monkeys produced by gene transfer into early-cleavage-stage embryos using a simian immunodeficiency virus-based vector. Proc Natl Acad Sci U S A 2010; 107: 17663-17667.
[16] Mazzini L, Mareschi K, Ferrero I, Vassallo E, Oliveri G, Boccaletti R, Testa L, Livigni S and Fagioli F. Autologous mesenchymal stem cells: clinical applications in amyotrophic lateral sclerosis. Neurol Res 2006; 28: 523-526.
[17] Chernykh ER, Shevela EY, Leplina OY, Tikhonova MA, Ostanin AA, Kulagin AD, Pronkina NY, Muradov M, Stupak VV and Kozlov VA. Characteristics of bone marrow cells under conditions of impaired innervation in patients with spinal trauma. Bull Exp Biol Med 2006; 141: 117-120.
[18] Krampera M, Franchini M, Pizzolo G and Aprili G. Mesenchymal stem cells: from biology to clinical use. Blood Transfus 2007; 5: 120-129.
[19] Minguell JJ and Erices A. Mesenchymal stem cells and the treatment of cardiac disease. Exp Biol Med (Maywood) 2006; 231: 39-49.
[20] Griffin M, Iqbal SA, Sebastian A, Colthurst J and Bayat A. Degenerate wave and capacitive coupling increase human MSC invasion and proliferation while reducing cytotoxicity in an in vitro wound healing model. PLoS One 2011; 6: e23404.
[21] Sasaki M, Abe R, Fujita Y, Ando S, Inokuma D and Shimizu H. Mesenchymal stem cells are recruited into wounded skin and contribute to wound repair by transdifferentiation into multiple skin cell type. J Immunol 2008; 180: 2581-2587.
[22] Kode JA, Mukherjee S, Joglekar MV and Hardikar AA. Mesenchymal stem cells: immunobiology and role in immunomodulation and tissue regeneration. Cytotherapy 2009; 11: 377-391.
[23] Garcia-Castro J, Trigueros C, Madrenas J, Perez-Simon JA, Rodriguez R and Menendez P. Mesenchymal stem cells and their use as cell replacement therapy and disease modelling tool. J Cell Mol Med 2008; 12: 2552-2565.
[24] Morandi F, Raffaghello L, Bianchi G, Meloni F, Salis A, Millo E, Ferrone S, Barnaba V and Pistoia V. Immunogenicity of human mesenchymal stem cells in HLA-class I-restricted T-cell responses against viral or tumor-associated antigens. Stem Cells 2008; 26: 1275-1287.
[25] Giuliani M, Oudrhiri N, Noman ZM, Vernochet A, Chouaib S, Azzarone B, Durrbach A and Bennaceur-Griscelli A. Human mesenchymal stem cells derived from induced pluripotent stem cells down-regulate NK-cell cytolytic machinery. Blood 2011; 118: 3254-3262.
[26] Spaggiari GM, Capobianco A, Becchetti S, Mingari MC and Moretta L. Mesenchymal stem cell-natural killer cell interactions: evidence that activated NK cells are capable of killing MSCs, whereas MSCs can inhibit IL-2-induced NK-cell proliferation. Blood 2006; 107: 1484-1490.